Groundwater

Groundwater Quality in the Yucatan Peninsula: Insights from Stable Isotope and Metals Analysis

by F. Arcega-Cabrera[1], J. O. Sickman[2], L. Fargher[3], J. Herrera-Silveira[4], D. Lucero[2], I. Oceguera-Vargas[1], E. Lamas-Cosío[1], and P. A. Robledo-Ardila[5]

Abstract

High surface water-groundwater connectivity characterizes watersheds underlain by karsts, increasing contaminant transport risks. However, karsts are highly complex, making research necessary to understand the transport of contaminants from the surface, through the aquifer, to discharge areas. In Yucatan, the lack of waste water treatment raises the risk of groundwater contamination. We monitored stable isotopes ($\delta^{18}O$-NO_3 and $\delta^{15}N$-NO_3), cadmium, and lead to document waste water contamination and transport during the rainy and dry seasons, using water samples collected along the Ring of Cenotes during each season. Specific conductance and pH showed no consistent seasonality, with conductance ranging from 0.5 to 55 mS/cm and pH ranging from 6.6 to 8.6 for most samples. Nitrate concentrations in the cenotes averaged $205 \pm 260\ \mu M$ and no seasonal pattern was observed. Cd and Pb concentrations were 0.1 to 37.9 µg/L and 0.2 to 243.2 µg/L, respectively. Nitrate stable isotope values were 2.6 to 27.2‰ for $\delta^{18}O$ and 1.2 to 20.7‰ for $\delta^{15}N$. The statistical relationship between $\delta^{15}N$ and $\delta^{18}O$, in dry season samples, indicated that denitrification was occurring. A scale measure for waste water recognition showed: (1) high variability among sites probably related with dry/rainy seasons and/or diverse anthropogenic activities; and (2) specific water quality variables that contribute to contamination at each site during each season. Importantly, our analyses indicate that in the area surrounding the Ring of Cenotes, waste water exhibits spatial and temporal patterns related to complex transport and dilution processes, as is the case in karsts in general.

Introduction

Groundwater contributes the majority of urban and agricultural water in Mexico (INEGI 2015) and long-term monitoring of aquifers, including more recent satellite-based measurements, indicates moderate to severe conditions of groundwater overuse (Castellazzi et al. 2016). Groundwater contamination caused by deficient waste water treatment and lack of correct solid-waste disposal is also an increasing problem in Mexico, where rapid economic and demographic growth has promoted accelerated environmental degradation (Arcega-Cabrera et al. 2014a, 2014b, 2017, 2018; Camacho-Cruz et al. 2019). Sustainable use of existing groundwater supplies, along with protection of groundwater from human-made pollutants is essential for water security in Mexico.

In the karstic landscape of the Yucatan Peninsula, this situation is particularly acute because surface water is absent, and groundwater is the main source for human use. Here, groundwater contamination and flow are strongly affected by a massive hydrologic formation, the Ring of Cenotes (RC), which is a semicircular arc characterized by a high density of flooded dolines or cenotes (Figure 1) (Pérez-Ceballos et al. 2012). These karstic formations intercept the water table (Gaona-Vizcayno et al. 1980) and are capable of transporting anthropogenic pollutants from inland areas toward coastal urban areas (Arcega-Cabrera et al. 2014a; Derrién et al. 2015). High connectivity between the land surface and karst aquifers increases the risk of domestic and industrial waste waters penetrating

[1]Corresponding author: Unidad de Química Sisal, Facultad de Química, Universidad Nacional Autónoma de México. Puerto de Abrigo Sisal, Yucatán, 97355 Mexico; +1-52-9992426939; farcega@unam.mx

[2]Department of Environmental Sciences, University of California, Riverside, 900 University Avenue, Riverside, CA, 92521; james.sickman@ucr.edu; delores.lucero@ucr.edu

[3]Ecología Humana, Cinvestav del IPN—Unidad Mérida, Km 6 antigua carretera a Progreso, Mérida, Yucatán 97310, Mexico; frederick.fargher@cinvestav.mx

[4]Recursos del Mar, Cinvestav del IPN—Unidad Mérida, Km 6 antigua carretera a Progreso, Mérida, Yucatán, 97310, Mexico; jorge.herrera@cinvestav.mx

[5]Instituto Geológico y Minero de España, Unidad del IGME en las Islas Baleares, Calle Feliciá Fuster No. 7, Palma de Mallorc, Baleares 07006, España; pa.robledo@igme.es

Article impact statement: Stable isotope and metals analysis of groundwater in Yucatan furthers research on waste water transport and dilution in karst aquifers.

Received November 2020, accepted May 2021.

doi: 10.1111/gwat.13109

groundwater (Miller 1990; Marín et al. 2000; Villasuso and Méndez-Ramos 2000; Pacheco et al. 2001; Arcega-Cabrera and Fargher 2016).

Systematic surveys of water quality in the RC to assess levels of contamination and the safety of water for human consumption are scarce. Moreover, very few studies have utilized techniques such as stable isotopes and trace element analysis to identify contamination sources, inorganic contaminants, model their transport and fate, and assess water-quality risk (Katz and Griffin 2008; Tziritis 2010; Albertin et al. 2011; Edwards et al. 2013; Arcega-Cabrera et al. 2014a). Inorganic groundwater contaminants, like nitrate and heavy metals, are relatively straightforward to measure using these techniques and their presence indicates a likelihood that other, more toxic organic contaminants are also entering urban water supplies in Yucatan.

Nitrate is a common contaminant in groundwaters of the Yucatan Peninsula (Saint-Loup et al. 2018) and levels are often high enough to potentially cause human illnesses ($>714\,\mu$mol/L), including infant methemoglobinemia (Fan and Steinberg 1996), cancer, endocrine disease, and birth defects (Ward et al. 2018). Non-point sources of nitrate, including runoff containing agricultural fertilizers, human waste, and waste from confined animal feeding operations, likely contribute the majority of the nitrogen found in the Yucatan's groundwater (Spalding and Exner 1993; Wakida and Lerner 2005). Accordingly, the N and O isotopes of nitrate have been used to understand sources of nitrate in the groundwater of karst aquifers (Albertin et al. 2011), while nutrients have been used to show direct waste water contamination mainly in coastal lagoons of Mexico (Herrera-Silveira et al. 2004; Herrera-Silveira and Morales-Ojeda 2009). Metals have been used in both areas to investigate contamination (Vesper and White 2003; Arcega-Cabrera et al. 2014a, 2014b, 2017, 2018).

In this study, we present inorganic water quality data, including pH, dissolved oxygen (OD), electric conductivity (EC), oxidation-reduction potential (ORP), nutrients, dual isotope analysis of NO_3^-, and cadmium, lead and strontium concentrations, from groundwater samples collected in the area surrounding the RC. This area is a region of high ecosystem and socioeconomic relevance in the Yucatan peninsula of Mexico. Our main objective was to establish relationships between waste water inputs, from agro-industrial areas and human settlements in the RC, with contaminant levels, as well as study the impact of the karstic environment on physicochemical processes and transport of contaminants. Moreover, using these water quality data in a multivariate environmental assessment, we mapped groundwater quality in the RC region. Our regional environmental assessment contributes to broader understanding of the fate of contaminated groundwater in karsts. It also provides a value tool that could be used by stakeholders to implement sustainable groundwater management practices in the Yucatan peninsula.

Study Area

The Yucatan Peninsula contains a well-developed karst system of interconnected fractures, joints, and solution openings (Marín et al. 2000). A dominant landscape feature is the semicircular concentration of flooded cenotes, known as the RC (Figure 1), which extends in an arc running southeast from Celestun (on the northwest coast of Yucatan) to Cuzama (in the interior of the state) and northeast from Cuzama to Dzilam (on the northeast coast of Yucatan) and is delineated by the Chicxulub impact crater (Pérez-Ceballos et al. 2012). The Yucatan peninsula possesses a tropical climate (26.3 °C mean annual air temperature) and experiences a rainy season from June to September, a "Nortes" season, characterized by strong winds from the north (from October to December), and a dry season (DS) from December to May. Mean annual precipitation is 1000 to 1200 mm (Graniel et al. 1999). Groundwater flow responds strongly to precipitation timing, with a velocity of 1×10^{-5} cm/s in the DS that climbs to 3 cm/s in the rainy season (Arcega-Cabrera et al. 2014). Economically and demographically, the RC area has experienced a significant increase in human population over the last 20 to 30 years, escalating the production of solid waste and waste water with relatively little treatment (SEMARNAT 2018).

Research Methods

Cenote Sampling

In May 2014 (DS) and October 2014 (wet season), water samples were collected with a Van Dorn bottle (depth = 0.5 m) from 32 hydrological features (Figure 1). Water samples for metals analyses were placed into acid-washed high-density polypropylene (HDPE) bottles, acidified to pH 2, using trace-metal grade HNO_3 and refrigerated at 5 °C until analysis (Arcega-Cabrera and Fargher 2016). Samples for NO_3^- concentration and isotopic analyses ($\delta^{15}N$ and $\delta^{18}O$ of NO_3^-) were filtered using 0.45 μm polycarbonate filters into clean HDPE bottles and stored frozen. Electrical conductivity (EC), dissolved oxygen (OD), and depth were measured in situ using a YSI Model 85 (with 3 m cable); pH and ORP were measured in the field using a Mettler Toledo FG2.

Chemical Analyses

The elements Cd, Pb, and Sr were analyzed by atomic absorption spectrophotometry (Perkin Elmer AAnalyst 800/FIAS 100 CDMX, CDMX, Mexico), using the graphite furnace technique for Cd and Pb, and the air-acetylene flame technique for Sr. Certified reference material NIST SRM 1640a (trace elements in natural water) was included in each analytical run to measure analytical accuracy, and duplicate samples were run to estimate analytical precision. Analytical accuracy, precision, and detection limit were 0.52%, 0.8%, and 0.01 μg/L for Cd; 4.95%, 0.7%, and 0.05 μg/L for Pb; and 0.55%, 0.8%, and 0.06 μg/L for Sr. Metal concentrations

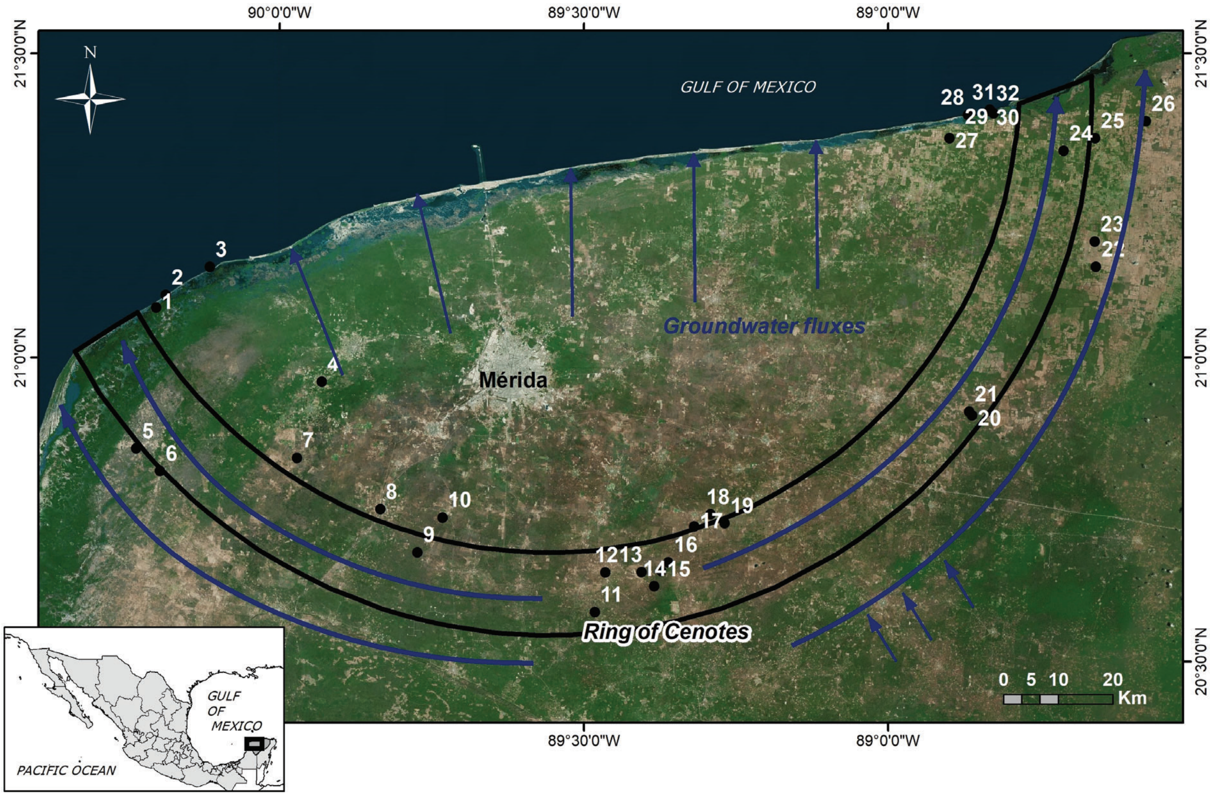

Figure 1. Study area showing the area of higher cenote abundance, known as the Ring of Cenotes (RC), main groundwater fluxes, and sampling sites.

were compared with the recommended values (RV) from Mexican norm *NOM-127-SSA1-1994 (5 μg/L for Cd and 25 μg/L for Pb) (the NOM lacks recommended values for Sr). Nitrate-NO_3 (μmol/L) was determined by cadmium reduction as described by Strickland and Parsons (1972). Nitrate concentration was compared with water quality standards in Mexico's NOM-127-SSA1-1994 (714.3 μmol/L).

To determine the $\delta^{15}N$ and $\delta^{18}O$ values of NO_3^-, the bacterial (*Pseudomonas aureofaciens*) denitrifier method (Coplen et al. 2012) was performed at the facility for isotope ratio mass spectrometry (FIRMS) at the University of California, Riverside. The $\delta^{15}N$ and $\delta^{18}O$ values were measured using a Thermo Delta V isotope ratio mass spectrometer with a GasBench injector. The international reference materials USGS-32, USGS-34, and USGS-35 were included in each analytical run. Values are expressed in permil units relative to atmospheric N_2 or Vienna Standard Mean Ocean Water (VSMOW).

Statistical Analyses and Integrative Environmental Assessment

Non-parametric statistics and multivariate analyses were performed using StatSoft STATISTICA program and JMP v.14. Data were transformed (log [1 + data]) to avoid magnitude or variable type bias. Significant differences were obtained with a Mann-Whitney U test ($p = 0.05$) to determine if the samples were drawn from the same distribution. Cluster analyses were carried out using Ward's method with a Pearson correlation (for example see Arcega-Cabrera et al. 2014a, 2014b). Since Factor analyses was used to measure the ratio of an item's unique variance to its shared variance, any item with a communality score of less than 0.2 was removed. A cut off value of 0.6 for significant loadings was used for sample sizes less than 100, following MacCallum et al. (1999).

Groundwater Quality Mapping

We used ArcGIS to map metal and nitrate concentrations relative to Mexican water quality standards. Values more than 10% below recommended concentrations are color-coded in green, those from 9.9% to 0.1% below in yellow, and those that are equal to or exceed them in red. For the nitrate isotope data, we inferred the presence of N from septic/manure sources when the $\delta^{15}N$ value exceeded 10‰ (Wang et al. 2014); we used green for absence and red for presence.

To construct the waste water recognition map, which shows the location of waste water based on its components, we used: (1) an ordinal code with zero units for green, one unit for yellow, and three units for red; and (2) we summed the values for each component (Cd + Pb + nitrate + $\delta^{15}N$ [from fertilizers or septic and manure]) to create a latent construct or scale measure of waste water contamination based on the NOM's recommended values. Therefore, possible scores range from 0 (least contaminated) to 12 (most contaminated).

Table 1
Characteristics of Sampled Sites

Site	Geographic Coordinates	Karst Feature Type	Maximum Depth (m)	Land Use
1	21°04′53.9″N 90°12′10.5″W	Cenote/Mangroves	48.7	Tourism/Fishing
2	21°06′08.5″N 90°11′1.6″W	Submerged discharge	4.0	None
3	21°08′54.7″N 90°06′52.3″W	Submerged discharge	4.6	None
4	20°57′35.4″N 89°55′49.6″W	Cenote	3.5	Tourism
5	20°51′00.9″N 90°14′08.0″W	Cenote	39.3	Town water supply
6	20°48′47.9″N 90°11′46.8″W	Cenote	14.0	Water supply for cattle
7	20°50′04.5″N 89°58′16.5″W	Cave	4.5	Tourism
8	20°45′00.8″N 89°50′03.7″W	Cave	3.7	Tourism
9	20°40′25.1″N 89°46′23.0″W	Cenote	5.0	Tourism
10	20°44′11.3″N 89°43′55.4″W	Cenote	10.0	None
11	20°34′50.6″N 89°28′52.4″W	Cenote	1.3	None
12	20°38′46.9″N 89°27′50.8″W	Cave	1.9	Town water supply
13	20°38′47.4″N 89°24′16.6″W	Cenote	25.7	Tourism
14	20°37′23.8″N 89°23′03.1″W	Cenote	10.0	Tourism
15	20°38′55.6″N 89°22′20.9″W	Cenote	45.0	Tourism, scuba
16	20°39′45.5″N 89°21′39.7″W	Cenote	52.3	Tourism
17	20°43′17.5″N 89°19′05.8″W	Cenote	0.5	Tourism
18	20°44′29.6″N 89°17′28.6″W	Cave	0.6	Tourism
19	20°43′37.2″N 89°16′05.3″W	Cenote	10.0	Tourism
20	20°54′15.2″N 88°51′41.7″W	Cenote	13.3	Water supply for cattle
21	20°54′37.5″N 88°51′59.0″W	Cenote	14.1	None
22	21°08′54.7″N 90°06′52.3″W	Cenote	48.0	Town water supply
23	21°11′24.0″N 88°39′34.7″W	Cenote	55.7	None
24	21°20′21.3″N 88°42′38.5″W	Cenote	13.3	None
25	21°21′35.2″N 88°39′33.4″W	Cenote	29.7	Water supply for cattle
26	21°23′16.8″N 88°34′31.3″W	Cenote	14.2	None
27	21°21′36.0″N 88°53′55.4″W	Cenote	0.3	Garbage deposit
28	21°23′54.5″N 88°52′06.0″W	Submerged discharge	4.0	None
29	21°24′02.1″N 88°49′33.2″W	Cenote / mangroves	5.2	Tourism
30	21°24′16.6″N 88°49′52.0″W	Submerged discharge	1.9	None
31	21°24′23.9″N 88°49′55.4″W	Submerged discharge	2.2	None
32	21°24′18.3″N 88°48′53.1″W	Submerged discharge	2.2	Tourism

Note: Maximum depth is the average of depth measurements made in May and October 2014.

Results

Characteristics, Land Use, and Physicochemical Conditions

The 32 sampling sites were selected to capture the wide variability of karst surface features in the Yucatan peninsula (Table 1). These features include: (1) submerged groundwater discharges or SGDs (18.8%); (2) cenotes (68.7%); and (3) caves (12.5%). Maximum depth to water table at the sites ranged from 0.3 to 55.7 m with mean and median depths of 15.3 and 7.6 m, respectively. About 19% of the karst features sampled are used for water supply, either for humans, cattle, or both; 44% are used for recreational activities such as swimming or diving; 34% are undeveloped; and, one site, the shallowest, is used as a garbage dump.

Anthropogenic activities are common in areas adjacent to the sampled sites (Figure 2). Crop production for animal feed occupies the largest area, followed by crops for human consumption. Rural settlements (<2500 inhabitants) are dispersed throughout the study area; whereas, urban areas (>2500 inhabitants) are located mainly in the north, near the Gulf of Mexico.

We observed little difference in specific conductivity between the dry and rainy seasons (Figure 3A), which parallels findings by Pérez-Ceballos et al. (2012). The central part of the RC shows a mean conductivity of 2 mS/cm, whilst the coastal cenotes and SGDs show conductivities around 30 mS/cm. This spatial pattern is observed for both seasons and, in particular, variations in sites 29 and 31 are likely related to their type (see Table 1). Site 29 is a coastal cenote with a constant fresh groundwater inlet and site 31 is a SGD with flux velocities as high as 1634 L/s (Kantún 2011).

Dissolved oxygen (Figure 3B) is highly variable across the cenotes and depends on the productivity, flow, and type of water body. Dissolved oxygen was lower during the rainy season in nearly all cenotes, probably because of increased terrestrial organic matter input followed by its aerobic degradation (Herrera-Silveira and Comín 2000).

Some differences ($p = 0.05$) in pH can be observed between the dry and rainy season values, with the largest differences occurring in the RC's northwestern sites (Figure 3C). More acidic waters are expected in lentic cenotes, owing to higher productivity and respiration,

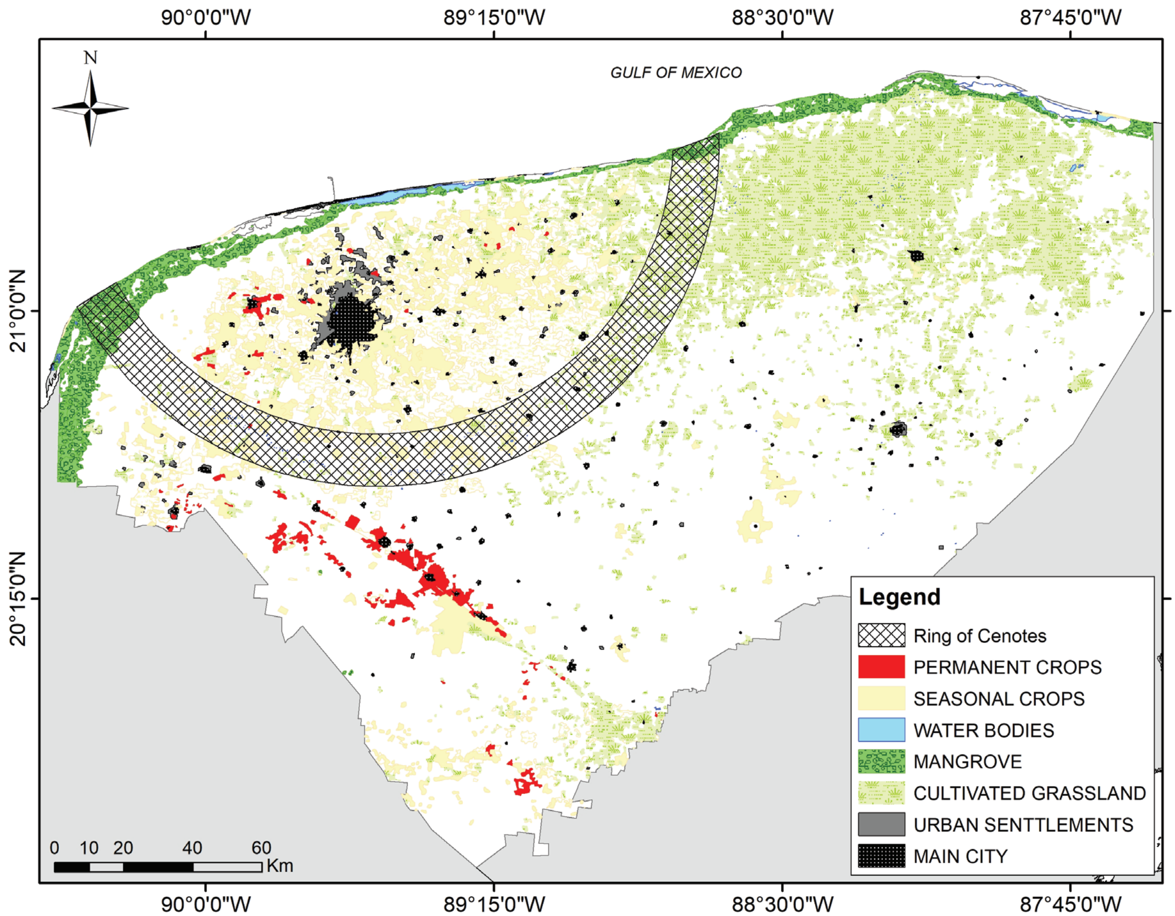

Figure 2. Map of land use in Yucatan with the Ring of Cenotes overlaid (adapted from Arcega-Cabrera et al. 2014a).

and also in coastal zones, because of the formation of H_2S under anoxic conditions (Herrera-Silveira and Comín 2000). Infiltrating water is expected to acquire CO_2 from the soil and from the oxidation of organic matter, contributing to decreases in the concentration of O_2 and increases in acidity, which in turn is partially neutralized by the dissolution of limestone. These processes could also be related with the ORP variations (Figure 3D), which show significant differences ($p = 0.05$) between the dry and rainy seasons, with much lower ORP during the rainy season. Therefore, the RC shows significant physicochemical variations between seasons, which is related to water and organic matter entering the system. Yet, it also shows significant differences between coastal and inland cenotes in terms of EC.

Waste water Recognition

Isotopes (δ^{18}O-NO_3 and δ^{15}N-NO_3), nitrate (NO_3), Cd, and Pb were quantified to identify the presence of waste water in cenotes and denitrification (Table 2). They were, also, coded to construct a scale measure of waste water recognition (Tziritis 2010).

Cadmium levels ranged from 0.1 to 37.9 µg/L and averaged 4.8 ± 9.9 µg/L. These values varied substantially between the dry and rainy seasons in some cenotes, but no statistically significant seasonal differences were observed (Figure 4A). There were nine instances of Cd exceeding the water quality standard, and, in three sampling sites (1, 3, and 28), the standard was exceeded in both seasons. Lead concentrations ranged from 0.2 to 243.2 µg/L and averaged 69 ± 82 µg/L. Concentrations were generally lower during the DS, but the difference is not significant. Six sites have Pb levels below the detection limit (Figure 4B). Lead concentrations exceeded the standard in 10 instances, with three sites exceeding the standard in both seasons (1, 2, and 3). Concentrations of Cd and Pb show significant correlations among the sampling sites, especially during the RS (DS Spearman's $\rho = 0.592$, $p < 0.001$, $n = 32$; RS Spearman's $\rho = 0.721$, $p < 0.0001$, $n = 32$); nevertheless, none of the sites with high concentrations of metals had nitrate levels that exceeded the water quality standard.

Nitrate concentrations in the sampling sites ranged from 0.7 to 1277 µM and averaged 205 ± 260 µM. There were four instances of nitrate exceeding the Mexican water quality standard in the DS and one in the rainy season. We observed no significant difference in the concentration of nitrate between the rainy and DSs (Figure 4C).

The stable isotope composition of nitrate in the sites was quite variable (Table 2). The δ^{18}O of nitrate varied from 2.6 to 27.2‰ with an average of 10.5 ± 5.4‰;

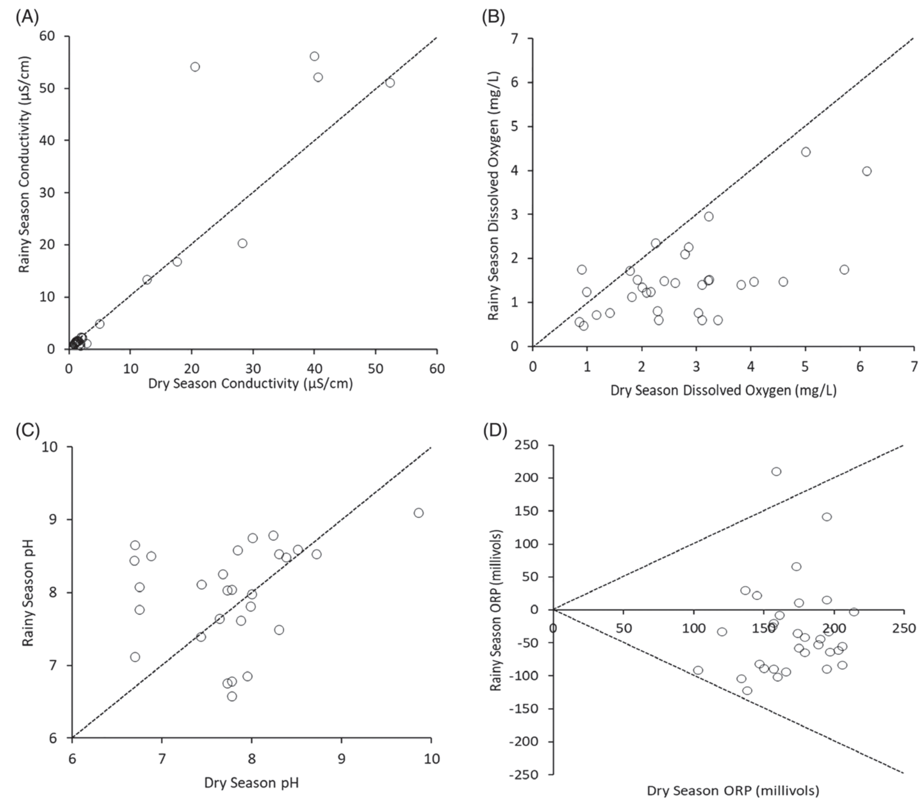

Figure 3. Physicochemical parameters variations in selected sites of the ring of cenotes (RC) for the dry season (DS) and rainy season (RS): (A) conductivity, (B) dissolved oxygen, (C) pH, and (D) ORP (oxidation-reduction potential). Line represents a 1:1 relation.

values above 20‰ suggest the presence of nitrate from atmospheric deposition (rain or dry deposition). The $\delta^{15}N$ of nitrate ranged from 1.2 to 20.7‰ and averaged 10.6 ± 3.3‰. Values above 10‰ suggest the presence of nitrate derived from human/animal sources, whereas values above 15‰ have been correlated with the presence of human pharmaceuticals and personal care products in California (Huang et al. 2012). Because of the overlap in $\delta^{15}N$ values between fertilizers and natural soil-derived NO_3, we interpreted $\delta^{15}N$ values between 1 and 10‰ to indicate a mixture of nitrate sources. There were more than 25 instances of $\delta^{15}N$ exceeding 10‰ and 8 instances where it exceeded 15‰. Some of the cenotes with high metal concentrations also had high $\delta^{15}N$ values, but relatively high $\delta^{15}N$ was also observed in cenotes with very low or undetectable metals concentrations. Similarly, we did not observe a strong coherence between the $\delta^{15}N$ of nitrate and nitrate concentrations (except in site #12). Cenotes with high nitrate concentrations often had $\delta^{15}N$ values between 8 and 11‰, indicating a variety of nitrate sources. The lack of strong coherence between metals and indices of nitrate contamination could be indicating that N contamination is predominately from diffuse non-point sources (Huang et al. 2012) in the sampling sites. Given the karstic nature of the study area, this pattern may be expected (Pacheco and Cabrera 1997; Pacheco et al. 2001; Katz and Griffin 2008; Albertin et al. 2011). Although, further research should be done to corroborate this.

In the DS (Figure 5A), there are 18 sites that exhibit isotopically enriched nitrate, suggesting the presence of waste water. Whilst in the rainy season (Figure 5B), the number decreases to 10. The sites in the southwest, northwest, and northeast sections of the RC show a constant presence, whilst the southeast section shows waste water presence only in site 19, and only in the DS. The presence of waste water may be linked to nearby anthropogenic activities (cf. Jiang et al. 2009), since $\delta^{15}N$ values suggest N from septic/manure and fertilizer origins. But at coastal sites, it is highly probable that waste water is transported as part of groundwater from southern sites. This groundwater behavior was reported before by Arcega-Cabrera et al. (2014a) and Derrién et al. (2015) using fecal sterols as waste water tracers. Waste water absence in the SE part of the RC, in the rainy season, could be related to relatively large groundwater flux (dilution) that has been reported to be as high as 1634 L/s (Kantún 2011). The flux increase could be promoting a washing effect during the rainy season that dilutes groundwater, transporting it faster and farther than in the DS. This is also shown in the northeast sites, where the waste water scale measurement changes from 9 in the rainy season to 1 in the DS. This groundwater behavior depends on the way variation in the water table affects transport through conduits or fractures, with higher transport during the rainy season.

Table 2
Isotope, Nitrate, Cd, and Pb Data During the Dry (DS) and Rainy Seasons (RS)

Sampling site	$\delta^{18}O$-NO_3 vs. VSMOW (‰)		$\delta^{15}N$-NO_3 vs. VSMOW (‰)		Cd, μg/L		Pb, μg/L		NO_3, μM	
	DS	RS	DS	RS	DS	RS	DS	RS	DS	RS
1	27.2	17.4	1.2	8.7	**15.2**	**32.2**	**94.1**	**203.4**	0.8	3.1
2	15.8	14.3	**13.0**	**11.5**	**9.8**	**37.9**	**110.1**	**184**	6.0	17.7
3	21.7	17.1	**18.6**	**15.8**	**34.5**	**33.2**	**135.9**	**211**	12.1	98.3
4	11.0	5.6	**13.2**	**10.7**	0.5	ND	ND	ND	434.6	338.3
5	10.8	11.6	**11.0**	8.3	0.3	ND	ND	ND	2.9	2.6
6	17.6	9.7	9.5	**10.8**	0.4	0.4	ND	2.9	12.0	0.7
7	8.3	5.1	9.0	8.1	0.5	0.4	1.4	ND	**859.7**	149.8
8	6.4	4.4	9.8	**11.2**	0.1	0.1	ND	ND	303.8	332.2
9	6.2	5.0	7.6	8.5	0.2	0.1	ND	ND	470.3	247.9
10	8.4	5.2	8.7	8.8	0.1	ND	ND	ND	**778.7**	270.9
11	13.9	6.3	8.9	8.3	0.5	ND	ND	ND	3.6	14.8
12	14.8	4.5	**15.3**	**14.5**	0.1	0.1	ND	ND	117.4	**872.8**
13	8.1	5.1	**11.2**	7.9	ND	0.4	ND	ND	**793.0**	248.8
14	6.0	4.8	7.3	8.3	0.1	0.1	0.2	ND	583.2	213.9
15	8.7	5.0	7.6	7.1	0.1	0.1	0.3	ND	74.5	175.8
16	6.6	4.8	7.5	7.0	0.2	0.6	0.2	2.4	157.4	195.5
17	6.9	5.0	7.2	8.1	0.2	0.1	0.2	ND	223.9	217.9
18	8.1	5.0	**10.8**	**11.4**	0.2	0.1	0.4	ND	**1277.4**	526.9
19	15.3	6.5	**11.3**	**20.7**	0.1	0.1	0.4	ND	487.2	235.9
20	7.3	11.6	**11.0**	9.9	0.1	ND	ND	ND	16.8	13.7
21	12.2	16.2	**15.6**	**11.4**	0.1	ND	ND	ND	3.3	26.9
22	9.4	16.0	**12.6**	5.7	0.1	ND	ND	ND	373.5	18.3
23	17.1	15.6	9.1	7.8	ND	0.8	4.9	ND	4.1	2.6
24	15.2	21.2	**11.1**	**11.9**	ND	0.5	ND	ND	8.3	1.3
25	10.3	14.7	**15.0**	**10.6**	0.1	0.1	ND	ND	120.4	0.9
26	19.2	22.7	**18.7**	9	ND	0.5	ND	ND	11.0	13.0
27	3.7	2.6	**14.0**	**16.1**	0.4	0.3	ND	ND	6.8	5.1
28	8.5	8.8	**10.5**	**11.5**	**9.95**	**14.4**	18.4	**60.0**	377.9	182.5
29	7.4	8.2	9.8	**10.1**	ND	1.5	ND	ND	236.7	215.8
30	7.9	8.0	**10.5**	**11.9**	3.6	0.1	**133.7**	ND	261.1	168.5
31	13.5	8.6	**13.7**	8.3	**19.1**	3.0	**243.2**	20.2	29.7	77.8
32	11.2	7.7	**11.9**	9.0	**22.0**	3.2	**156.4**	5.1	98.1	89.7

ND = below the detection limit.

Notes: Values in bold are above the national or international recommended values. Recommended values for Cd (5 μg/L), Pb (15-25 μg/L), and nitrates (714.3 μM) were taken from NOM-127-SSA1-1994, WHO (1993), and SQuiRTs (Buchman 2008); $\delta^{18}O$-NO_3 vs. VSMOW (‰) values >20 indicate presence of atmospheric NO_3, $\delta^{15}N$-NO_3 vs. VSMOW (‰) values >10 indicate presence of human/animal waste.

Nitrate contamination could be related with the agro-waste water input, mainly in the central and southwestern portions of the RC, where the use of agrochemicals has been reported (SEDUMA 2012). For nitrate, it seems that nitrate reduction by microorganisms is promoting low levels in almost all sites in the RC area.

During the DS, we did not detect a relationship between anthropogenic activities and metal concentrations. This despite the fact that Cd and Pb have been previously related with agricultural and domestic waste water (Graniel et al. 1999). Cadmium and Pb were generally higher in coastal sites, where their concentrations exceed SQuiRTs values (Buchman 2008). This could be an indication that SGDs are sources of metals along the coast. Arcega-Cabrera et al. (2014b) reported this same process for fecal matter, using fecal sterols and stanols as tracers. Pacheco and Cabrera (1997) showed that metal presence (mainly Cd) in inland regions, happens only in events of significantly increased groundwater flux, like in heavy storms or hurricanes. This pattern is probably related to metals being retained in the karstic matrix or co-precipitating with organic material (Arcega-Cabrera et al. 2010). Therefore, it is probable that higher metal levels in the coastal area are the product of long-distance transport and concentration in the groundwater.

The waste water scale measure demonstrates that contamination related to anthropogenic activities is present in the RC area and shows significant differences between the dry and rainy seasons related with concentration and dilution processes. Transport of waste water to the coast of Yucatan could be contributing to the degradation of sensitive habitats, like mangroves and coastal lagoons, or even the incidence of toxic microorganisms (Herrera-Silveira and Morales-Ojeda 2009; Hernández-Terrones et al. 2011; Arcega-Cabrera et al. 2014a; Hernández-Terrones et al. 2015; Kantún-Manzano et al. 2018).

Denitrification can be discerned by examining the relationship between the $\delta^{15}N$ and $\delta^{18}O$ values of

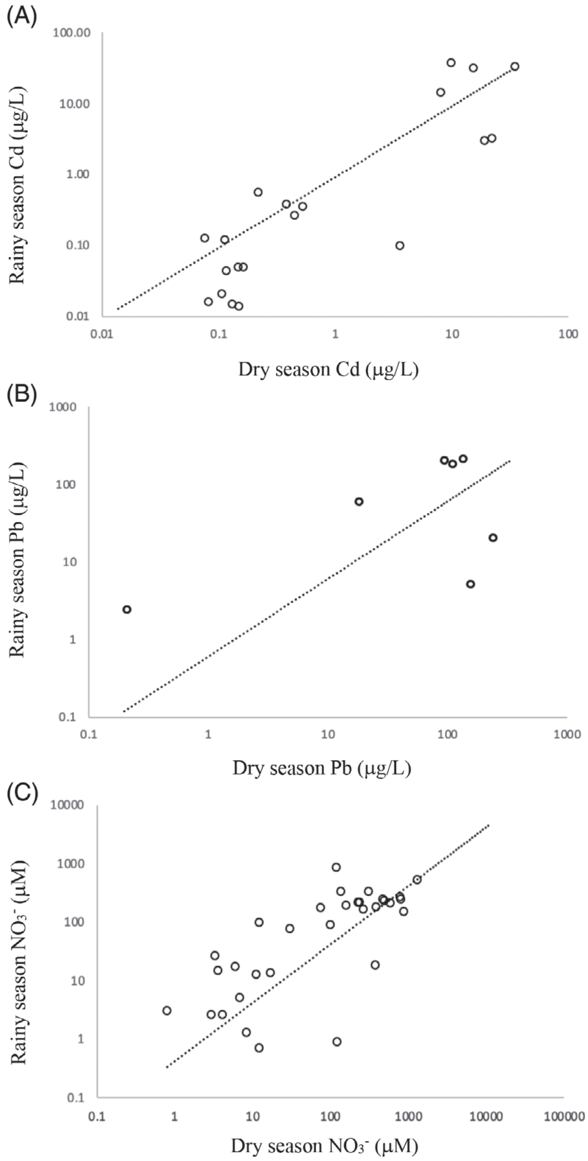

Figure 4. Concentrations of metals and nitrate in selected sites for rainy season (RS) and dry season (DS): (A) Cd; (B) Pb; (C) nitrate.

nitrate and by observing the relationship between δ ^{15}N-NO_3 and nitrate concentration (Kendall and McDonnell 1998; Albertin et al. 2011; Huang et al. 2012). When denitrification is occurring in an aquifer, fractionation will leave a characteristic isotope effect on the remaining nitrate in the aquifer, typically leading to a linear relationship between δ ^{15}N and δ ^{18}O values with a slope of approximately ±0.5 ($y = \delta\,^{18}O$, $x = \delta\,^{15}N$). In addition, as nitrate is microbially reduced, one should observe an inverse relationship between nitrate concentration and δ ^{15}N-NO_3, as the residual nitrate pool shrinks, but becomes progressively isotopically enriched due to kinetic fractionation caused by denitrification. During the DS, we detected a linear relationship between δ^{15}N-NO_3 and δ ^{18}O-NO_3 (Figure 6A; $R^2 = 0.30$; p = 0.001) and an inverse relationship was discernable between nitrate concentrations and δ^{15}N-NO_3 (p = 0.069). The 95% confidence interval for the slope of the line in Figure 6A ranged from 0.34 to 1.25, encompassing the characteristic slope of 0.5 caused by denitrification. No relationship was observed during the rainy season (Figure 6B) between δ ^{15}N-NO_3 and δ ^{18}O-NO_3 or between δ ^{15}N-NO_3 and nitrate concentration. It is likely that the longer residence time of water in the aquifer during the DS allows the isotopic effects of denitrification to be detected. Whereas, during the rainy season, new inputs of nitrate from the surface obscure the effects of denitrification. While denitrification is likely occurring in most cenotes, the fact that nitrate concentrations exceed established standards suggests that the rate of contamination of some of the sampled cenotes exceeds the rate of natural removal of nitrate, through denitrification, leading to unsafe nitrate concentrations at those sites.

Multivariate Analyses

Cluster analyses by season are presented in Figure 7A and 7B. In the DS, three groups can be observed, moving from left to right in the diagram. The first one groups all stations with waste water input. This group shows a significant distance from the others, demonstrating the relevance of waste water input for these sites. The second group denotes sites free from waste water input and with low water conductivity. The last group is composed of sites with high conductivity and no waste water input.

For the rainy season (Figure 7B), sites in the NW area of the RC remained grouped (S1, 2, and 3), but the grouping for the rest of the sites changes. Although sites with waste water input remain grouped (middle group), some other sites, free of waste water, occur in this group. This could be the result of the significant flux increment in the intricate karstic system, promoting the mixing of different water masses that are not in contact during the DS due to the aquifer's low flux. It could also be showing a dilution process, since fewer sites show waste water input; or, it could be the result of transport to coastal areas. Cracks and conduits can change the general flow pattern in a given area, and a given site could show higher seasonal variation (White 1988) depending on its connection with the aquifer (Herrera-Silveira and Comín 2000).

In order to further understand the variables contributing to the variability of waste water presence in the RC, integrative environmental assessment was used (Morales-Caselles et al. 2008a, 2008b; Bonnail et al. 2016). Results can be observed in Figure 8.

Table 3 shows the factor analysis for dry and rainy seasons that explains approximately 80% of the total variance. For the DS, three factors were extracted. Factor 1 loads metals (Cd and Pb) inversely with EC and Sr. Strontium and EC are directly correlated since they indicate brackish/salt water presence. An inverse correlation between Cd/Pb and Sr./EC indicates that metals inputs to the RC are related with the groundwater system and processes, such as input from the hydrological basin, rather than from a saline intrusion (Arcega-Cabrera et al. 2014a). Factor 2 groups nitrate inversely with pH and ORP. This could be indicating nitrate reduction in

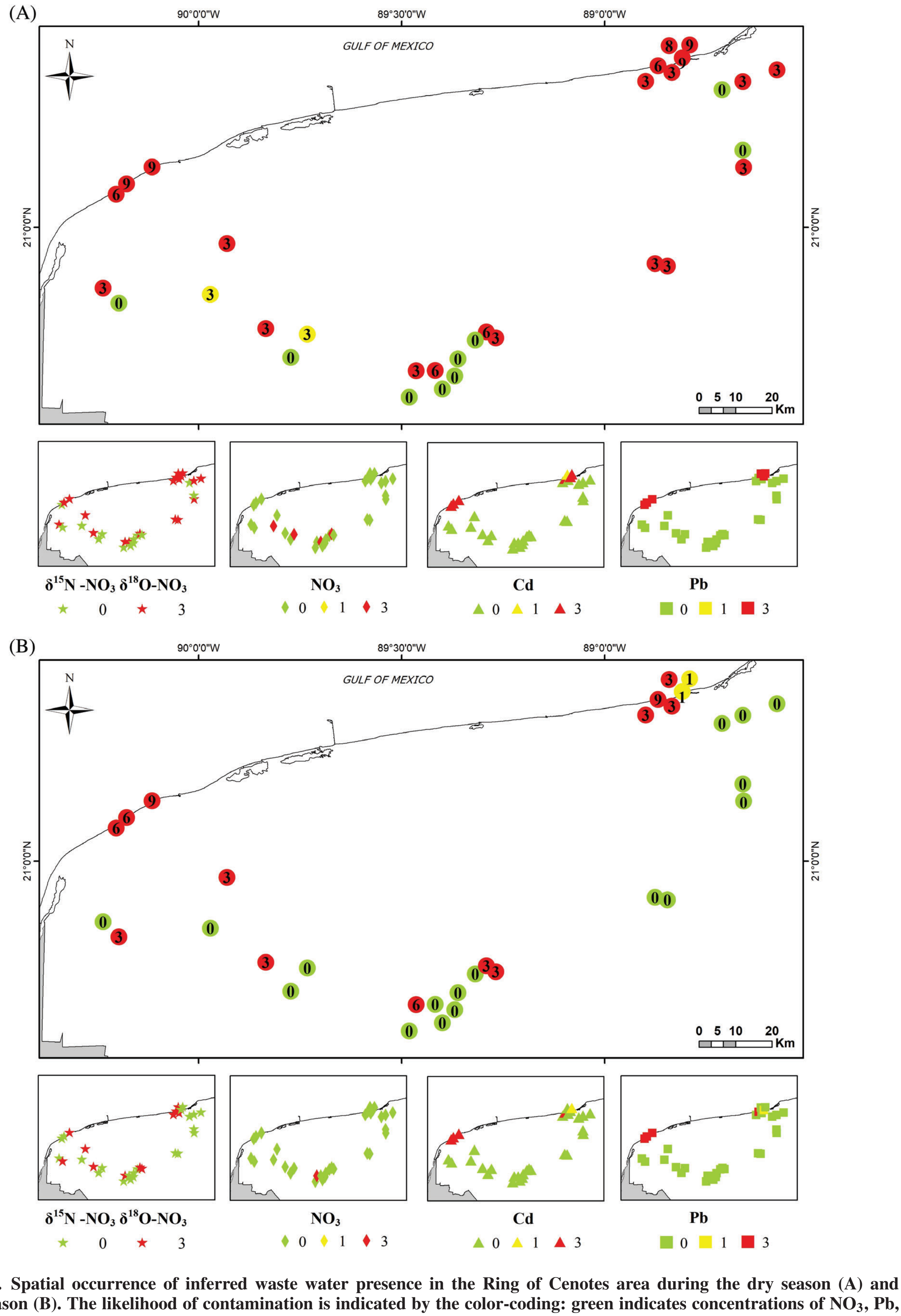

Figure 5. Spatial occurrence of inferred waste water presence in the Ring of Cenotes area during the dry season (A) and rainy season (B). The likelihood of contamination is indicated by the color-coding: green indicates concentrations of NO_3, Pb, and Cd that are 10% or more below the Mexican water quality standard; yellow where concentrations of NO_3, Pb, and Cd are 9.9% to 0.1% below this standard, and red where δ15N values exceed the standard (10‰) and concentrations of NO_3, Pb, and Cd ≥ water quality standard.

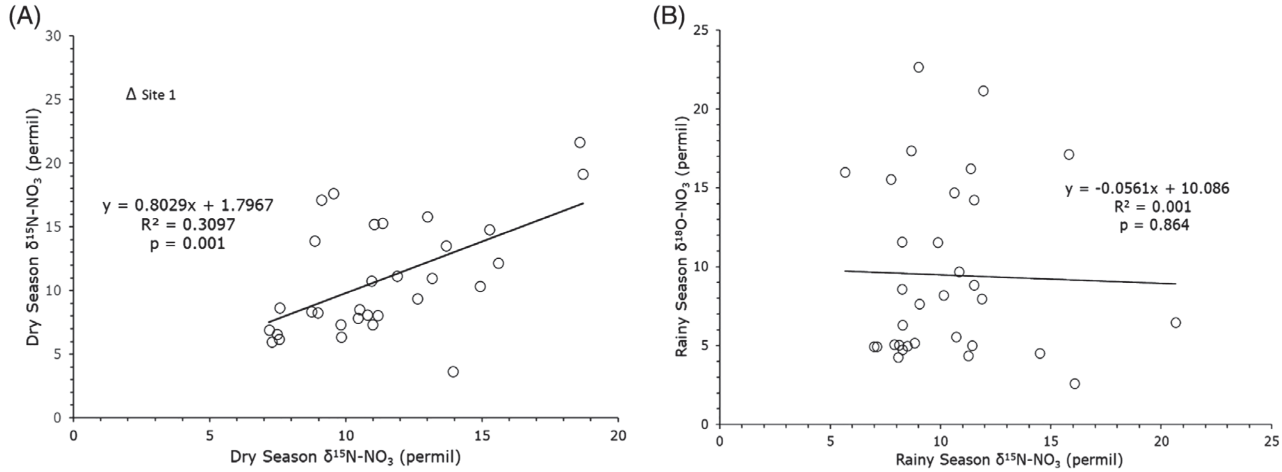

Figure 6. Isotope biplot for cenotes sampled in the dry and rainy seasons. Site 1 was an outlier and not included in the regression for the dry season.

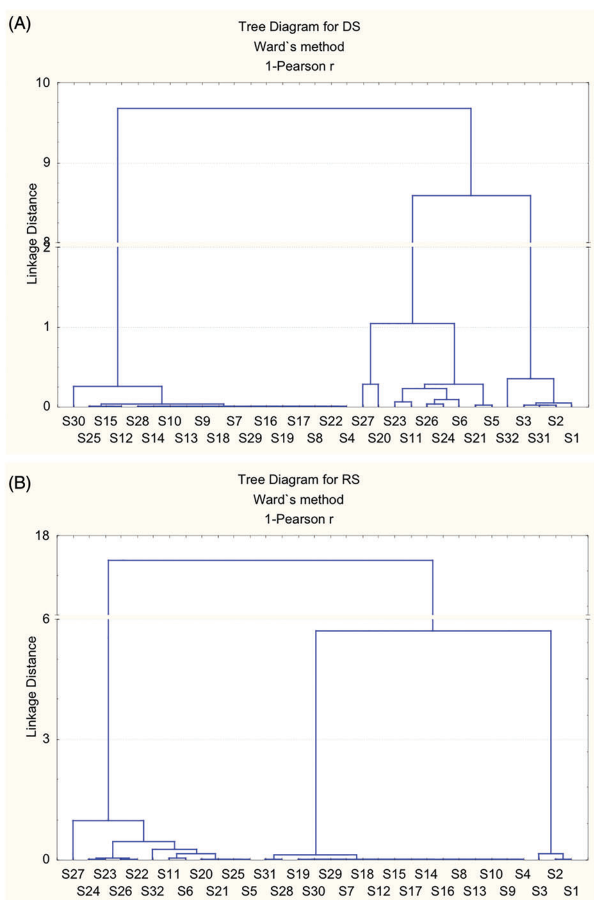

Figure 7. Cluster analysis: (A) dry season (DS) and (B) rainy season (RS) at the Ring of Cenotes (RC).

a more acidic and reductive environment, such as would be expected for groundwater. Factor 3 groups nitrate with isotopes, which indicates waste water presence, mainly related with septic tanks or manure.

For the rainy season, three factors, that explain about 80% of the total variance, were also extracted. The first one groups metals inversely with EC and Sr., as was the case in the DS, showing that the presence of metals in groundwater does not depend on hydrological variations and, instead, input is constant and related with in situ sources. Factor 2 groups inversely pH with ORP and could be indicating the presence of rain water in the groundwater system. Factor 3 groups isotopes with nitrate and dissolved oxygen. This third factor could be indicating nitrogen input related with waste water from septic tanks or manure (groundwater has a lower oxygen content

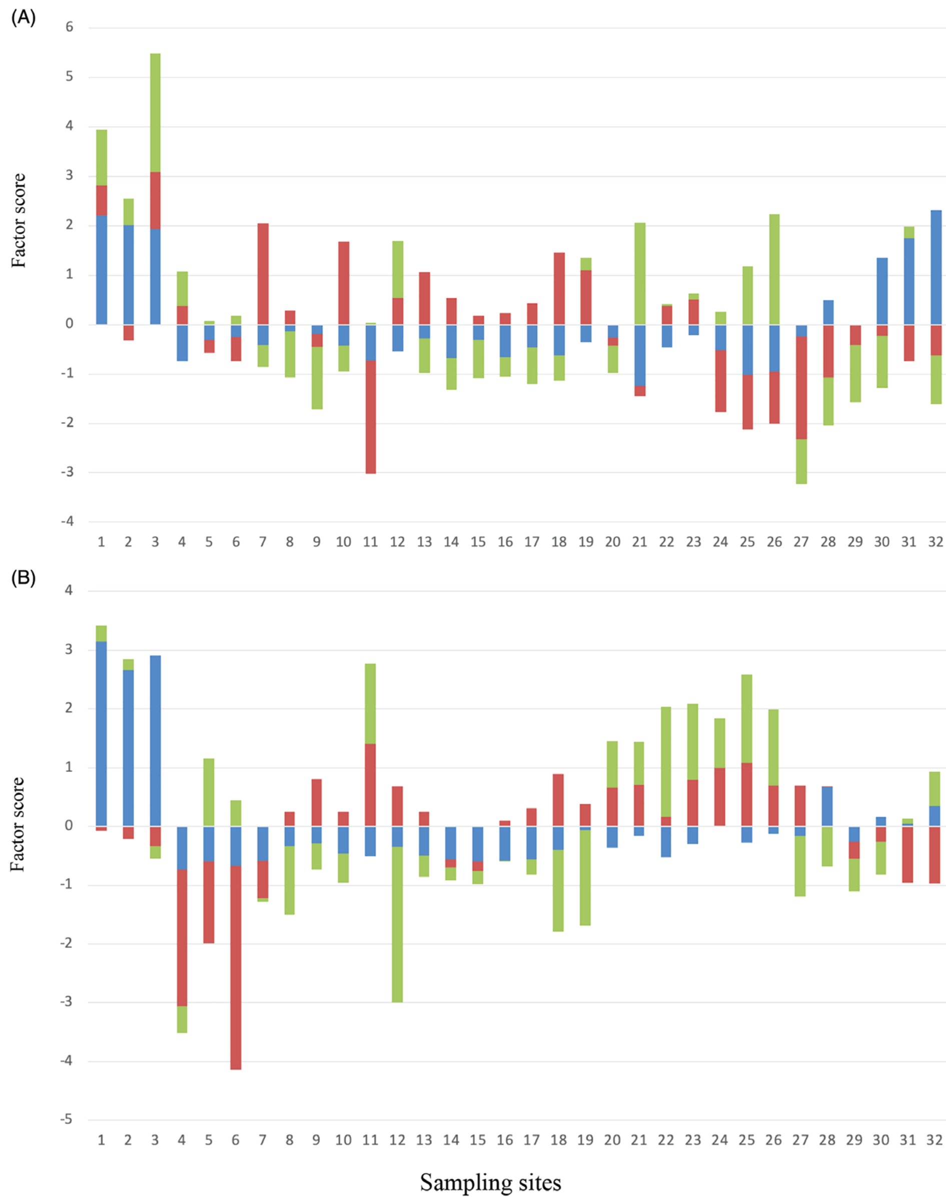

Figure 8. Site specific factor scores in dry season (A) and rainy season (B). F1 = factor 1 in blue color (groundwater metals); F2 = factor 2 in red color (nitrate input); F3 = factor 3 in green color (N from septic/manure).

compared with rain water), as well as from runoff from the hydrological basin, which is probably injecting nitrogen from agrochemicals. Therefore, waste water presence in the RC depends on the hydrological season, being more significant in the rainy season.

Hydrological-dependent behavior was analyzed for each site, since each one could be affected in a different manner by its geological context and nearby sources. Results (Figure 8A and 8B) show that metals input is relevant at sites 1, 2, 3, 28, 30, 31, and 32, which are the sites of SGDs. Consequently, these sites are functioning as sources of metals in coastal areas (Arcega-Cabrera et al. 2014a, 2014b; Derrién et al. 2015; Kantún-Manzano et al. 2018).

Factor 2 is significant in the sites located along the central part of the RC area, where agriculture activities dominate. Thus, it suggests that nitrate could be related to input from agrochemicals.

Factor 3, which represents waste water input with N from septic tanks or manure, is significant in sites 1, 2, 3, and 32, which are most of the SGDs, showing that these sites are also functioning as sources of waste water in the coastal area. These results concur with results previously reported by Arcega-Cabrera et al. (2014a), Derrién et al. (2015), and Kantún-Manzano et al. (2018), which identified fecal matter input from SGDs. Also, sites that are near human settlements, ranches, or used for touristic activities show a significant score on factor 3 (sites 11, 12, 20, 21, 22, 23, 24, 25, and 26; see Figure 8B and 8C). It is noteworthy, as well, that these same sites show a higher factor 3 score in the rainy season than in the DS, corroborating the influence of hydrology in waste water variation in the RC.

Table 3
Factor Analysis for Dry and Rainy Seasons

	Dry season			Rainy season		
	F1	**F2**	**F3**	**F1**	**F2**	**F3**
15N-NO_3	0.2	−0.2	**0.8**	0.3	0.1	**0.6**
18O-NO_3	0.4	0.1	**0.7**	0.5	0.1	**0.7**
NO_3	−0.3	**0.6**	−0.4	−0.2	0.1	**0.8**
Cd	**0.8**	0.1	0.4	**0.9**	−0.1	0.1
Pb	**0.9**	−0.1	0.1	**0.9**	−0.1	0.1
EC	**−0.9**	−0.1	0.1	**−0.9**	−0.2	0.1
DO	−0.5	−0.5	0.4	0.2	0.4	**0.6**
pH	−0.2	**−0.8**	0.2	0.2	**0.9**	0.1
ORP	−0.2	**−0.8**	0.2	0.1	**−0.9**	0.1
Sr	**−0.9**	0.1	0.2	**−0.9**	−0.1	0.1
Expl Var	3.6	1.9	1.8	3.9	2.1	1.8
Prp Totl	0.4	0.2	0.2	0.4	0.2	0.2

EC = electrical conductivity, DO = dissolved oxygen, ORP = oxidation-reduction potential, Expl Var = explained variability, Prp Totl = proportionality total.
Note: Significant values are bold. F1 = factor 1, F2 = factor 2, F3 = factor 3.

Conclusions

Human development in a complex karstic aquifer often affects the environment, mainly through contamination. But seasonal changes in general flow patterns make it more difficult to identify those sites that are affected by anthropogenic activities. Using several indicators to construct a scale measure for waste water recognition, it was possible to identify waste water input and its qualitative magnitude and to relate it with nearby anthropogenic activities. A multivariate analysis showed significant seasonal changes that could be the result of incremented flow during the rainy season, promoting dilution and transport of waste water mainly from the interior to the coast where sensitive ecosystems, such as mangroves, are located. Isotopes also showed that the rate of contamination of the aquifer exceeds the rate of natural removal of nitrate, leading to unsafe concentrations of nitrate. The integrative environmental assessment corroborated the presence of waste water in several cenotes, even those used for human provisioning. It also showed the variables contributing to contamination at each site. Although the map gives a useful overview of the distribution and behavior of anthropogenic contamination, the mobility inferred from concentration changes corresponds to the sampling year and concentrations may vary from year to year. In addition, the determination of other contaminants should be included to assess the constraints and potential general application of the index. Nevertheless, this map could be used as a practical tool to inform stakeholders regarding contamination in other karstic areas.

Acknowledgments

The authors wish to thank UNAM-PAPIIT IA101914 and UNAM-PAIP 5000-9146 for funding. We thank Alejandra Martínez Escamilla for project administration, and the reviewers for their insightful remarks that significantly improve the quality of the article.

Authors' Note

The authors do not have any conflicts of interest or financial disclosures to report.

References

Albertin, A., J.O. Sickman, A. Pinowska, and R.J. Stevenson. 2011. Identification of nitrogen sources and transformations within karst springs using isotope tracers of nitrogen. *Biogeochemistry*, 134 pp. https://doi.org/10.1007/s10533-011-9592-0

Arcega-Cabrera, F., L. Fargher, M. Quesadas-Rojas, R. Moo-Puc, I. Oceguera-Vargas, E. Noreña-Barroso, L. Yáñez-Estrada, J. Alvarado, L. González, N. Pérez-Herrera, and S. Pérez-Medina. 2018. Environmental exposure of children to toxic trace elements (Hg, Cr, As) in an urban area of Yucatan, Mexico: Water, blood, and urine levels. *Bulletin of Environmental Contamination and Toxicology* 100, no. 5: 620–626. https://doi.org/10.1007/s00128-018-2306-8

Arcega-Cabrera, F., L.F. Fargher, I. Oceguera-Vargas, E. Noreña-Barroso, L. Yáñez-Estrada, J. Alvarado, L. González, R. Moo-Puc, N. Pérez Herrera, M. Quesada-Rojas, and S. Pérez-Medina. 2017. Water consumption as source of arsenic, chromium, and mercury in children living in rural Yucatan, Mexico: Blood and urine levels. *Bulletin of Environmental Contamination and Toxicology* 99, no. 4: 452–459. https://doi.org/10.1007/s00128-017-2147-x

Arcega-Cabrera, F., and L.F. Fargher. 2016. Education, fish consumption, well water, chicken coops, and cooking fires: Using biogeochemistry and ethnography to study exposure of children from Yuctan, Mexico to metals and arsenic. *Science of the Total Environment* 568: 75–82.

Arcega-Cabrera, F., N. Velázquez-Tavera, L. Fargher, M. Derrien, and E. Noreña-Barroso. 2014a. Fecal sterols, seasonal variability, and probable sources along the ring of cenotes, Yucatan, Mexico. *Journal of Contaminant Hydrology* 168: 41–49.

Arcega-Cabrera, F., R. Garza-Pérez, E. Noreña-Barroso, and I. Oceguera-Vargas. 2014b. Impacts of geochemical and environmental factors on seasonal variation of heavy metals in a coastal lagoon Yucatan, Mexico. *Bulletin of Environmental Contamination and Toxicology* 94: 58–65.

Arcega-Cabrera, F., S.E. Castillo-Blum, and M.A. Armienta. 2010. Tetraethyl lead kinetics: Release from sediments in a mine impacted tropical river. *Revista Internacional de Contaminación Ambiental* 2, no. 26: 119–127.

Bonnail, E., A.M. Sarmiento, and T.A. DelValls. 2016. The use of a weight-of-evidence approach to address sediment quality in the Odiel River basin (SW, Spain). *Ecotoxicology and Environmental Safety* 133: 243–251.

Buchman, M.F. 2008. NOAA Screening Quick Reference Tables, NOAA OR&P Report 08-1, Seattle WA, Office of Response and Restoriation Division, National Oceanic and Atmospheric Administration 34 pp.

Camacho-Cruz, K.A., M.C. Ortiz-Hernández, A. Sánchez, L. Carrillo, and A. De Jesús Navarrete. 2019. Water quality in the eastern karst region of the Yucatan peninsula: Nutrients and stable nitrogen isotopes in turtle grass, *Thalassia testudinum*. *Environmental Science and Pollution Research* 27, no. 14: 15967–15983. https://doi.org/10.1007/s11356-019-04757-3

Castellazzi, P., R. Martel, and A. Rivera. 2016. Groundwater depletion in Central Mexico: Use of GRACE and InSAR to support water resources management. *Water Resources Research* 52: 5985–6003.

Coplen, T.B., Q. Haiping, K. Révész, K. Casciotti and J.E. Hannon. 2012. Determination of the δ15N and δ18O of nitrate in water; RSIL lab code 2900, chap. 17 of Stable isotope-ratio methods, sec. C. of Révész, Kinga and Coplen, T.B. Eds. *Methods of the Reston Stable Isotope Laboratory (Slightly Revised from Version 1.0 Released in 2007)*: 12201 Sunrise Valley Drive Reston, VA 20192, USA: U.S. Geological Survey Techniques and Methods, 35. https://pubs.usgs.gov/tm/2006/tm10c17/. Accesed May 2020.

Derrién, M., F. Arcega-Cabrera, N. Velázquez, C. Kantún-Manzano, and S. Capella. 2015. Sources and distribution of organic matter along the Ring of Cenotes, Yucatan, Mexico: Sterol markers and statistical approaches. *Science of the Total Environment* 511: 223–229.

Edwards, A., M. Devendra, M. Thomas, H. Williams, and J. April. 2013. Flow characterization in the santee cave system in the chapel branch creek watershed, upper coastal plain of South Carolina, USA. *Journal of Cave and Karst Studies* 75, no. 2: 136–145. https://doi.org/10.4311/2011ES0262

Fan, A.M., and V.E. Steinberg. (1996) Health implications of nitrate and nitrite in drinking water: an update on methemoglobinemia occurrence and reproductive and developmental toxicity. *Regulatory Toxicology and Pharmacology*, 23, no. 1: 35–43. http://dx.doi.org/10.1006/rtph.1996.0006.

Gaona-Vizcayno, S., T. Gordillo de Anda, and M. Villasuso-Pino. 1980. Cenotes, karst característico: Mecanismos de formación. *UNAM, Instituto de Geología* 4, no. 1: 32–36.

Graniel, C.E., L.B. Morris, and L.B. Carrillo-Rivera. 1999. Effects of urbanization on groundwater resources of Merida, Yucatan, Mexico. *Environmental Geology* 37, no. 4: 303–312.

Hernández-Terrones, L., K.A. Null, D. Ortega-Camacho, and A. Paytan. 2015. Water quality assessment in the Mexican Caribbean: Impacts on the coastal ecosystem. *Continental Shelf Research* 102, no. 1: 62–72.

Hernández-Terrones, L., M. Rebolledo-Vieyra, M. Merino-Ibarra, M. Soto, A. Le-Cossec, and E. Monroy-Ríos. 2011. Groundwater pollution in a karstic region (NE Yucatan): Baseline nutrient content and flux to coastal ecosystems. *Water, Air, and Soil Pollution* 218, no. 1–4: 517–528.

Herrera-Silveira, J.A., and S.M. Morales-Ojeda. 2009. Evaluation of the health status of a coastal ecosystem in southeast Mexico: Assessment of water quality, phytoplankton and submerged aquatic vegetation. *Marine Pollution Bulletin* 59: 72–86.

Herrera-Silveira, J.A., F.A. Comin, N. Aranda-Cirerol, L. Troccoli, and L. Capurro. 2004. Coastal waters quality assessment in the Yucatan Peninsula: Management implications. *Ocean & Coastal Management.* 47: 625–639.

Herrera-Silveira, J.A., and F.A. Comín. 2000. An introductory account of the types of aquatic ecosystems of Yucatan Peninsula (SE Mexico). In *Aquatic Ecosystems of Mexico: Status & Scope*. Ecovision World Monographs Series, ed. M. Munawar, S.G. Lawrence, I.F. Munawar, and D.F. Malley, 213–227. Leiden: Backhuys Pub.

Huang, W., J. Conkle, J.O. Sickman, and J. Gan. 2012. Water Quality Assessment of the Beaumont Management Zone: Identifying Sources of Groundwater Contamination Using Chemical and Isotopic Tracers. Final Report to the State Water Resources Control Board. University of California, Riverside SWRCB Agreement No. R8-2010-0022 Department of Environmental Sciences University of California Riverside, CA 92521, February 3, 2012: 93.

Instituto Nacional de Estadística y Geografía (INEGI). 2015. Encuesta Intercensal 2015, Mexico.

Jiang, Y., Y. Wu, and D. Yuan. 2009. Human impacts on karst groundwater contamination deduced by coupled nitrogen with strontium isotopes in the Nandong Underground River system in Yunan, China. *Environmental Science & Technology* 2009, no. 43: 7676–7683.

Kantún, M.C. 2011. Nutrient contribution by submerged groundwater discharges to the coastal zone of Dzilam de Bravo, Yucatan. CINVESTAV-Unidad Mérida. Master thesis. 120.

Kantún-Manzano, C., F. Arcega-Cabrera, M. Derrien, E. Noreña-Barroso, and J. Herrera-Silveira. 2018. Submerged groundwater discharges as source of fecal material in protected karstic coastal areas. *Geofluids* 3, no. 4: 1–11. https://doi.org/10.1155/2018/9736260

Katz, B.G., and D.W. Griffin. 2008. Using chemical and microbiological indicators to track the possible movement of contaminants from the land application of reclaimed municipal wastewater in a karstic springs basin. *Environmental Geology* 55: 801–821.

Kendall, C., and J.J. McDonnell. 1998. Chapter 16: Tracing nitrogen sources and cycling in catchment. In *Isotope Tracers in Catchment Hydrology*, 519–576. Amsterdam: Elsevier Science B.V.

MacCallum, R.C., K. Widaman, S. Zhang, and S. Hong. 1999. Sample size in factor analysis. *Psychological Methods* 4, no. 1: 84–99.

Marín, L.E., B. Steinich, J. Pacheco, and O.A. Escolero. 2000. Hydrogeology of a contaminated sole source karst aquifer: The case of Merida, Yucatan, Mexico. *Geofisica Internacional* 4: 12–18.

Miller, J.C. 1990. Relative vulnerability of the Floridan and Yucatecan aquifers to groundwater contamination. Extended Abstract, Simposio Internacional sobre Planeación, Menajo e Investigación de los Recursos Hidraúlicos. Universidad Autónoma de Yucatán, Mérida, Yucatán, México (January 24–26).

Morales-Caselles, C., I. Riba, C. Sarasquete, and T.A. DelValls. 2008a. The application of a weight of evidence approach to compare the quality of coastal sediments affected by acute (Prestige 2002) and chronic (Bay of Algeciras) oil spills. *Environmental Pollution* 156, no. 2: 394–402.

Morales-Caselles, C., I. Riba, C. Sarasquete, and T.A. DelValls. 2008b. Using a classical weight-of-evidence approach for 4 years monitoring of the impact of an accidental oil spill on sediment quality. *Environment International* 34: 514–523.

Pacheco, J., A. Cabrera, and L.E. Marín. 2001. Nitrate temporal and spatial patterns in twelve water supply wells, Yucatan, Mexico. *Environmental Geology* 40, no. 6: 708–715.

Pacheco, J., and S.A. Cabrera. 1997. Groundwater contamination by nitrates in the Yucatan Peninsula, Mexico. *Hydrogeology Journal* 5, no. 2: 47–53.

Pérez-Ceballos, R., J. Pacheco-Ávila, and H. Hernández-Arana. 2012. Regionalization based on water chemistry and physicochemical traits in the ring of cenotes, Yucatan, Mexico. *Journal of Cave and Karst Studies the National Speleological Society Bulletin* 74, no. 1: 90–102.

Saint-Loup, R., T. Felix, A. Maqueda, A. Schiller, and P. Renard. 2018. A survey of groundwater quality in Tulum region, Yucatan Peninsula, Mexico. *Environmental Earth Sciences* 77: 644. https://doi.org/10.1007/s12665-018-7747-1

SEDUMA. 2012. Secretaria de Desarrollo Urbano y Medio Ambiente. www.seduma.gob.mx

SEMARNAT. 2018. https://apps1.semarnat.gob.mx:8443/dgeia/informe15/tema/cap6.html#tema2

Spalding, R.F., and M.E. Exner. 1993. Occurrence of nitrate in groundwater—A review. *Journal of Environmental Quality* 22, no. 3: 392–402.

Strickland, J., and T. Parsons. 1972. A practical handbook of seawater analysis. *Bulletin of the Fisheries Research Board of Canada* 167: 310.

Tziritis, E. 2010. Assessment of NO_3 contamination in a karstic aquifer, with the use of geochemical data and spatial analysis. *Environment and Earth Science* (2010) 60:1381–1390 DOI https://doi.org/10.1007/s12665-009-0274-3.

Vesper, D.J., and W.B. White. 2003. Metal transport to karst springs during storm flow: An example from Fort Campbell, Kentucky/Tennessee, USA. *Journal of Hydrology* 276, no. 1: 20–36.

Villasuso, M., and R. Méndez-Ramos. 2000. A conceptual model of the aquifer of the Yucatan Peninsula. In *Population, Development, and Environment on the Yucatan Peninsula: From Ancient Maya to 2030.* ed. W. Lutz, L. Prieto, and W. Sanderson, IIASA Research Report. Laxenburg, Austria: RR-00-014: IIASA, pp. 120–139.

Wakida, F.T., and D.N. Lerner. 2005. Non-agricultural sources of groundwater nitrate: A review and case study. *Water Research* 39, no. 1: 3–16.

Wang, K.R., F. Guo, G.H. Jiang, and H.Y. Bian. 2014. Application of ^{15}N and ^{18}O to nitrogen pollution source in karst water in Eastern Guilin. *China Environmental Science* 34, no. 9: 2223–2230.

Ward, M.H., R.R. Jones, J.D. Brender, T.M. De Kok, P.J. Weyer, B.T. Nolan, C.M. Villanueva, and S.G. Van Breda. 2018. Drinking water nitrate and human health: An updated review. *International Journal of Environmental Research and Public Health* 2018, no. 15: 1557.

White, W.B. 1988. *Geomorphology and Hydrology of Karst Terrains*, Vol. 1988, 464. New York: Oxford University Press.

WHO. 1993. World Health Organization Nitrate and Nitrite guidelines. https://www.who.int/water_sanitation_health/dwq/chemicals/nitratenitrite2ndadd.pdf